International Journal for Parasitology: Parasites and Wildlife 24 (2024) 100944

Contents lists available at ScienceDirect

International Journal for Parasitology: Parasites and Wildlife

journal homepage: www.elsevier.com/locate/ijppaw

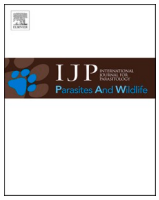

Description, life cycle, and development of the myxozoan *Myxobolus rasmusseni* n. sp. in fathead minnows, *Pimephales promelas*: A possible emerging pathogen in southern Alberta, Canada

Molly F. Tilley [a], Danielle Barry [b], Patrick C. Hanington [b], Cameron P. Goater [a,*]

[a] Department of Biological Sciences, University of Lethbridge, Lethbridge, AB, Canada, T1K 3M4
[b] School of Public Health, University of Alberta, Edmonton, AB, Canada, T6G 1C9

ARTICLE INFO

Keywords:
Myxospore
Triactinomyxon spores
TAM
18S rDNA gene
Emerging aquatic disease
Tubifex

ABSTRACT

Morphological, gene sequence, host tissue tropism, and life cycle characteristics were utilized to describe the myxozoan, *Myxobolus rasmusseni* n. sp. from fathead minnow, *Pimephales promelas,* collected from reservoirs in southern Alberta. Results from serial histological sections of whole heads showed that myxospores were contained within irregular-shaped and sized coelozoic capsules (=plasmodia). Clusters of membrane-bound, myxospore-filled plasmodia filled the head cavities of juvenile fathead minnows, leading to the development of large, white, disfiguring lesions in mid to late summer. Bilateral exopthalmia (pop-eye disease) was a common outcome of *M. rasmusseni* n. sp. development. BLASTn search of a 1974 bp sequence of the 18S rDNA gene isolated from myxospores indicated that *M. rasmusseni* n. sp. was distinct from other coelozoic and histozoic *Myxobolus* spp. cataloged in GenBank. 18S rDNA gene sequences from triactinomyxon spores released from the oligochaete *Tubifex* were 100% identical to sequences from myxospores collected from syntopic fathead minnows. Results from a longitudinal survey of the 2020 cohort of fathead minnows showed that young-of-the-year are exposed at 1–5 mo and that 60–90% of these had developed myxospore-filled lesions approximately one year later. Data regarding potential sources and timing of *M. rasmusseni* n. sp. emergence in fathead minnow populations are needed.

1. Introduction

The Myxozoa comprise a monophyletic taxa within the Phylum Cnidaria that have adopted a specialized endoparasitic life style (Chang et al., 2015). Of the approximately 2400 known species, almost all incorporate obligate development stages within both invertebrate (annelid or bryozoan) and vertebrate (typically fishes) hosts (review by Okamura et al., 2015). Whereas extensive research has been devoted to the evolutionary origins and radiation of these parasitic cnidarians, additional focus has been on their disease-causing potential, particularly in the context of the global expansion of aquaculture economies (Bartholomew and Kerans, 2015). Further recent focus has been on the extent, causes, and consequences of emergence and transmission of myxozoans within new host populations and into new host species where they can be an important threat to aquatic biodiversity and conservation (e.g. Carraro et al., 2017; James et al., 2021).

Characterizing and understanding the biodiversity of myxozoans remains an important challenge, made difficult by their small size, uniform morphology, and highly derived characters. Integration of life cycle information, ultrastructural morphometrics, host tissue-selection, and molecular sequencing approaches are often required to differentiate among the many seemingly cryptic species (Atkinson et al., 2015). Furthermore, the life cycles of many myxozoans are unresolved, making identification and interpretation of complex developmental stages difficult (Eszterbauer et al., 2015). Of the approximately 2400 known myxozoan species, only 60 have a partially described life cycle, and only 6 of which are routinely maintained under laboratory conditions (Fontes et al., 2015). Thus, 40 years after the initial life cycle confirmation of *Myxobolus cerebralis* (Markiw and Wolf, 1983), the causative agent of whirling disease in salmonid fishes, these important parasites of fishes remain enigmatic.

Compared to other cyprinid fishes in North America, the parasite assemblage of fathead minnows, *Pimephales promelas,* is relatively well characterized. This small-bodied forage fish tends to dominate fish

* Corresponding author.
E-mail address: cam.goater@uleth.ca (C.P. Goater).

https://doi.org/10.1016/j.ijppaw.2024.100944
Received 24 January 2024; Received in revised form 10 May 2024; Accepted 11 May 2024
Available online 27 May 2024
2213-2244/© 2024 The Authors. Published by Elsevier Ltd on behalf of Australian Society for Parasitology. This is an open access article under the CC BY-NC-ND license (http://creativecommons.org/licenses/by-nc-nd/4.0/).

communities in the shallow, eutrophic ponds and lakes that lack piscivorous predators in North America's northern Great Plains (Robinson and Tonn, 1989; Herwig et al., 2010). Although the assemblage tends to be dominated by several species of larval strigeoid trematodes that use piscivorous birds as definitive hosts (Sandland et al., 2001; Wisenden et al., 2012; Ahn, 2019; Hirtle et al., 2023), species of microsporidian, myxozoan, cestode, nematode and acanthocephalan are also frequently reported in the host survey literature. The results of previous research completed in our laboratory over the past 25 years has described numerous components of the parasite assemblages in fathead minnows at the northern edge of their range in Alberta, Canada (Sandland et al., 2001; Hirtle et al., 2023). Furthermore, annual host surveys have been completed at two targeted sites in this region since 2005 (Ahn, 2019). This extensive survey effort includes complete parasite censuses of approximately 2000 individual fathead minnows sampled across a broad spatial and temporal scale. In addition to providing information on spatial-temporal patterns of parasite transmission, the overall data set provides a benchmark that can be used to detect parasite extirpations and parasite introductions in this region, including those involving myxozoans.

During our routine sampling efforts involving fathead minnow populations in summer, 2017, large numbers of fathead minnows were observed with conspicuous white lesions/protrusions that were particularly obvious within circumorbital tissue (Fig. 1, Supplementary Content Video). These observations were made on fathead minnows at six of seven wetlands sampled that year, but not in prior years. The colour, shape, and location of the lesions were similar to those caused by some myxozoans in other species of fish (Lom and Dykova, 1992; Cone and Raesly, 1995; Frey et al., 1998; Ksepka et al., 2022). In the case of infected fathead minnows, the lesions were associated with distinctive exophthalmia (pop-eye disease) that was easily visible within schools of juvenile fish (Fig. 2; Supplementary Content Video). Microscopic examination of individual lesions revealed thousands of mature myxospores. Our initial determinations suggested that the myxospores were distinct from other fathead-infecting myxozoans (*Myxobolus hyborhynchi* Fantham, Porter and Richardson, 1939*, Myxobolus hendricksoni* Mitchell et al., 1985, *Unicauda magna* Minchew, 1981*, Myxobolus angustus* Kudo, 1934*), Myxobolus aureatus* Kudo (1934) and *Myxobolus hoffmanni* (Meglitsch, 1963) and other cyprinid-infecting myxozoans based on tissue tropism, spore morphology, and the presence of the conspicuous, disfiguring lesions.

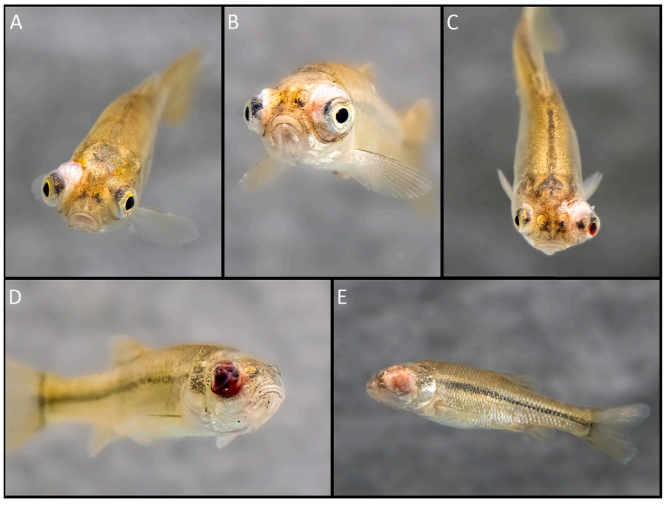

Fig. 1. Disfiguring lesions on the heads of 1-yr old fathead minnows infected with *Myxobolus rasmusseni* n. sp. Minnows were live-trapped from University Pond, Lethbridge, Ab in summer, 2022, placed into a single aquarium in the laboratory, then photographed with a digital camera. A) Unilateral exopthalmia of the right eye. B) Bilateral exopthalmia with additional lesions on dorsal surface of circumorbital cavity and on surface of left nares. C) Asymmetric exopthalmia of the left dorsal circumorbital cavity; hemorrhage within left vitreous humour, D) Severe hemorrhage of the right eye. E) Pathology of the epidermis of the left posterior circumorbital cavity and surface of left operculum.

Fig. 2. *In situ* image of a school of surfacing 1-yr old fathead minnows in University Pond, Lethbridge, Ab. Each minnow has bilateral or unilateral exopthalmia associated with infection of myxospore-containing plasmodia of *Myxobolus rasmusseni* n. sp. Note additional large, whitish lesions located on the anterior epidermal surface of some minnows.

In this study, we combine morphological and molecular approaches to describe *Myxobolus rasmusseni* n. sp. isolated from lesions located in and on the head region of fathead minnows collected from sites in southern Alberta. Our first objective is to combine morphological data, molecular sequence data, tissues site observations, and phylogenetic criteria, to describe *M. rasmusseni* n. sp. We next use molecular sequence data to identify the invertebrate alternate host in the life cycle of *M. rasmusseni* n. sp. To address this aim, we follow methods described in Székely et al. (2015) to match pairs of sequences of potentially conspecific developmental stages isolated from both fathead minnows and sympatric oligochaetes. Lastly, we use data from longitudinal host surveys of the 2020 fathead minnow cohort at two sites to estimate the timing of triactinomyxon spore transmission and the temporal patterns of lesion development.

2. Materials and methods

2.1. Host collection

We collected fathead minnows from 5 sites in southern Alberta (Table 1) where the characteristic lesions were obvious in fish observed from the shoreline (Figs. 1 and 2, Supplementary Content Video). The 5 sites were accessible by road and were located within 200 km of the University of Lethbridge. Sub-samples of fathead minnows collected

Table 1
Collection sites, sample sizes, and experimental endpoints for fathead minnows and tubificid worms collected in this study.

Collection site	Year	Host	n	Fate of hosts
University Pond	2018	Fathead minnow	10	preparation of host and parasite tissues
Bathing Lake, University Pond, CCSP[a]; SCR[b]	2018	Fathead minnow	12	histology
University Pond	2019	Fathead minnow	6	DNA sequencing of parasite tissue
University Pond	2019	Tubificid worms	10	DNA sequencing of parasite and host tissue
University Pond	2020	Fathead minnow	4	electron microscopy
Stirling Children's Pond	2021	Fathead minnow	2	histology

[a] Coulee Creek Stormwater Pond.
[b] Spruce Coulee Reservoir.

from the 5 sites provided the sources of parasite and host material for the histological, imaging, and molecular components of the work reported here (Table 1).

The seasonality of development of *Myxobolus*-induced lesions was evaluated by monitoring the visible presence of lesions in the 2020 cohort of fathead minnows at two additional sites, Coalhurst Stormwater Pond and McQuillan Reservoir. The sampling procedure followed methods modified from Heins et al. (2001) and was designed to estimate the timing of fathead minnow exposure to triactinomyxon spores (TAMs) and the timing of the duration of lesion development over the two-year life span of fathead minnows in this region. Longitudinal sampling of the 2020 cohort occurred at these two additional sites in fall 2020 (3–4 mo olds), spring 2021 (12–14 mo olds) and fall, 2021 (16–18 mo olds). During the fall, 2020 sample period, young-of-the-year (YOY) were collected using dip net sweeps from the shoreline. These samples were pooled into a single aerated container, from which samples were haphazardly removed (n = 50), photographed, and then released. Standard length of each YOY was assessed from the digital images with ImageJ. For the remaining two periods, fathead minnows were collected from overnight sets of 6 Gee minnow traps set along the shoreline approximately 2 m apart and at approximately 1.5 m depth (Sandland et al., 2001; Heins et al., 2001). All adults collected in each trap were pooled into a single aerated container. One hundred individuals were then haphazardly removed, measured for standard length, scored visually for the presence/absence of lesions on the body surface, and then released.

To document the alternate host of *M. rasmusseni* n. sp. we collected samples of oligochaete worms (n = 920) from University Pond on August 28, 2019. This site was selected for its high density of lesioned fathead minnows and for its high densities of tubificid worms. Collections involved 15, 30 s kick-samples taken with a hand-held freshwater sampling net. The samples were taken at haphazardly-selected locations approximately 1m apart along a 30 m stretch along the eastern edge of the pond. The contents of each sweep net were washed into a bucket, filtered through a 2 mm mesh, and then re-suspended into dechlorinated water. Tubificid worms were isolated from the bulk contents by eye, divided into subsets of ten worms, and left overnight in 3 ml of dechlorinated water. The subsets were then screened under a dissecting microscope for the presence of free-floating TAMs using crystal violet stain (Nehring et al., 2003). Subsets of worms that were confirmed to contain TAMs were then divided individually into vials with dechlorinated water.

2.2. Histological procedures

Following capture, live fathead minnows were transported to the University of Lethbridge where they were euthanized in concentrated MS-222 and immediately fixed in 10% neutral buffered formalin. Following a 3-day fixation period, the tip of the snout and a section located approximately 3 mm behind the anal fin was removed with a scalpel to ensure optimal penetration of the chelating agent, ethylenediaminetetraacetic acid (EDTA). The fish were then placed into 10% ethylenediaminetetraacetic acid to decalcify the bones (Matisz et al., 2010).

The fixed and decalcified fathead minnows were coronally-sectioned into 4 mm pieces and dehydrated, infiltrated with paraffin wax, and embedded into paraffin blocks (Matisz et al., 2010). The fish were sectioned at 5 μm using a microtome (American Optical Corporation "820" Spencer). Sections were mounted onto microscope slides and stained following Gill's 3 III Hematoxylin and Eosin Protocol (Cone and Frasca, 2002). The stained slides were sequentially viewed using light microscopy and imaged using Zeiss Axioskop Imager MI. Assessments of diagnostic morphological characters utilized MBF stereoinvestigator software and Image-J.

To evaluate the extent of *M. rasmusseni* n. sp. development within the host's head cavity, two additional fathead minnows with conspicuous lesions were sampled from Stirling Children's Pond (Table 1), fixed, and decalcified. The slides were stained using Harris Hematoxylin & Eosin staining (Leica Biosystems, 2022) and then imaged using Hamamatsu NanoZoomer 2.0RS and NDP.scan version 3.3.0 software.

2.3. Light and transmission electron microscopy

Ten juvenile fathead minnows with characteristic lesions were euthanized following the methods described above. First, a small section of lesioned tissue was removed from each fish. Wet smears were applied to the surface of a microscope slide, viewed with light microscopy (Zeiss Axioskop 40, Carl Zeiss Microimaging, Germany) and imaged using Canon Powershot A640. Myxospores (n = 50) from the fresh wet smears were measured for spore dimensions using an ocular micrometer. Dimensions measured were total spore length, total spore width, polar capsule length, polar capsule width, and the number of turns in the polar filament coil (Lom and Arthur, 1989). Preparations from the fresh wet smears were stained with methylene blue and imaged with Canon Powershot A640. Lugol's iodine was applied to representative slides of the smears and observed with light microscopy to determine the structure of the mucous coat surrounding individual myxospores and iodinophilous vacuoles and to determine the structure of sutural ridges (Liu et al., 2012).

To prepare host and parasite tissue for transmission electron microscopy (TEM), the circumorbital cavities of 4 lesion-bearing fathead minnows were isolated and placed into fresh Karnovsky's fixative for 24 h. The fixed tissue was transferred into 0.1% sodium cacodylate overnight (Matisz et al., 2010), post-fixed in cacodylate buffered (0.1M, pH 7.2) 1% osmium tetraoxide for 1 h then rinsed for 15 min in reverse osmosis water before dehydration through a graded ethanol series. Tissues were transitioned through a graded series of ethanol and propylene oxide and embedded into Epon resin (Matisz et al., 2010). The tissues were then cut at 60 nm on a Reichart OM-U2 ultramicrotome and stained with uranyl acetate and Reynold's lead citrate. The sections were imaged using an Hitachi TEM (acceleration voltage 100 kV) in the Central Analytical Facility at the University of Lethbridge.

2.4. DNA extraction, PCR, and sequencing

Myxobolus rasmusseni n. sp. DNA was extracted from tissue removed from 6 lesion-bearing fathead minnows collected from University Pond. Extraction procedures followed the manufacturer's instructions for the Qiagen DNeasy Blood and Tissue Kit. Two minor modifications from the instructions included an elution of 50 μl and a minimum digestion period of 2 h. DNA isolated from lesioned tissue was amplified using the ERIB1(sequence, 5′-ACCTGGTTGATCCTGCAG-3′) and ACT1r (sequence,

5′-AATTTCACCTCTCGCTGCCA-3′) primers from Hallet and Diamant (2001) and Barta et al. (1997) respectively, and the Myxgen4f (sequence, 5′-GTGCCTTGAATAAATCAGAG-3′) and ERIB10 (sequence, 5′-CTTCCGCGAGGTTCACCTACGG-3′) primers from Diamant et al. (2004) and Bartasova et al. (2009), respectively. The 2 primer sets produced two overlapping regions of the 18S rDNA gene. The initial PCR denaturation was 95° C for 3 min, followed by 35 cycles of 95° C for 30 s, 55 °C for 45 s, 72 °C for 1 min, 15 s, and the final elongation at 72 °C for 7 min. The product was run on 1% agarose gel and extracted with GeneJet Gel Extraction Kit.

We also extracted DNA from the suspensions of TAM's isolated from 10 infected tubificid worms collected from University Pond. Extraction procedures followed those described above except we included an elution of 50 µl and prior to tissue digestion, ethanol was removed by opening the microcentrifuge and allowing for evaporation for approximately 16 h. PCR reaction volumes were 12.5 µl, with 6.25 µl of 2X enzyme mix, 1 µl of nuclease free water, 5 µl DNA, and 125 nM primer concentrations. The thermocycler was run at: 95 °C for 3 min, followed by 45 cycles of 94 °C for 30 s, 55 °C for 45 s, 72 °C for 1 min and 15 s, and a final elongation at 72 °C for 7 min. The amplicons were run on a 1% agarose gel, extracted using the GeneJet Gel Extraction Kit.

PCR-amplified partial sequences of *COX1* gene from the Folmer region of the tubificid worms used 10 µl IDT PrimeTime master mix reaction volumes with 4 µl of extracted oligochaete DNA and LCO and HCO primers (Folmer et al., 1994) at 250 nM concentrations. Denaturing began with 95 °C for 5 min, followed by a series of cycles: 35 cycles of 95C for 40 s, 44 °C for 45 s, 72 °C for 1 min, with a final elongation of 72 °C for 8 min. Amplicon products obtained from amplification with the LCO and HCO primers were run on 1% agarose gel and subsequently extracted with the GeneJet Gel Extraction Kit. The purified amplicons produced using the same LCO and HCO primers, and ERIB1-ACT1r and Myxgen4f-ERIB10 primers, respectively. The amplicons were Sanger sequenced by Macrogen.

The sequence quality of oligochaete DNA was evaluated and trimmed using the 4peaks (Nucleobytes) software and snapgene viewer, and the primer regions were trimmed prior to alignment of the forward and reverse segments in Geneious Prime2019 (https://www.geneious.com, 2019). The contiguous sequence from each oligochaete sample was then compared against other cataloged species in the NCBI GenBank BLASTn database. Finally, each contiguous sequence was aligned with each representative species that shared greater than 80% sequence similarity to produce a percent identity matrix.

2.5. Phylogenetic analysis

We completed a BLAST search in GenBank to compare our consensus sequence with other submitted sequences. Those sequences that shared close genetic similarity with the consensus sequence of *M. rasmusseni* n. sp. as well as those of related *Myxobolus* spp. reported from 18 other cyprinids in North America, Europe, and southeast Asia were downloaded from GenBank following similar species selection described in McAllister et al. (2023). *Ceratonova* (=*Ceratomyxa*) *shasta* Noble, 1950 was selected as the outgroup. Myxozoan DNA sequences were aligned in MEGA 11.0, and manually edited to obtain a contiguous sequence of 1968 bp from the overlapping regions of the two 18S rDNA gene primer sets. We used CLUSTALW to align the 18S rDNA gene sequences. The sequences were manually edited in MEGA 11.0 which resulted in a 2102 bp alignment. Phylogenetic analyses using the general time reversible model (GTR + G + I) was determined by Akaike information criterion values in MEGA 11.0 and a maximum likelihood analysis was performed using all sites. The resulting tree was generated with 1000 confidence bootstrap estimates (Nei & Kumar, 2000). The tree was edited in Adobe Acrobat (Adobe, Inc., San Jose, CA, USA) to remove bootstrap values below 70% confidence.

3. Results

3.1. Description of *Myxobolus rasmusseni* n sp.

Family *Myxobolidae* Thélohan, 1892
Genus *Myxobolus* Bütschli, 1882
Myxobolus rasmusseni n. sp.

Type host: Fathead minnow *Pimephales promelas* Rafinesque, 1820 (Cypriniformes: Cyprinidae)

Type locality: University Pond, University of Lethbridge, Lethbridge, Alberta, Canada (49.680631, −112.870276)

Site of infection: Disfiguring lesions containing myxospore-filled plasmodia located primarily on surface of circumorbital sinus and oral cavities; secondarily on epithelial tissues associated with mandibular and opercular regions of head and pectoral girdle.

Type specimens: 1 syntype hematoxylin-stained histological slide and one formalin-preserved, fathead minnow with lesions deposited in the University of Alberta freshwater invertebrate collection, Edmonton, Canada under accession numbers #IN5001 (histological slide) and #IN5002 (whole fish). GenBank voucher PP375284, GenBank triactinospore voucher PP591956.

Prevalence: Prevalence: 92.3% of 196 1-yr old fathead minnows sampled from 5 reservoirs near Lethbridge, AB, Canada in July 2019 contained plasmodium-filled lesions.

Etymology: Species named after Dr. Joseph Rasmussen, Department Biological Sciences, University of Lethbridge, AB, Canada in recognition of his theoretical and empirical contributions to fisheries biology and aquatic ecosystem ecology.

3.1.1. Morphological description

Myxospores pyriform in valvular view, contained within various sized and shaped, membrane bound plasmodia (Figs. 3–5). Myxospores present within plasmodia as singles or couplets (Fig. 4A). Myxospore dimensions - 14.7–15.5 µm long (15.1 ± 0.4; n = 50) X 7.2–8.0 µm (7.6 ± 0.4; n = 50) wide. Myxospore comprised of two smooth symmetrical valves containing straight sutural ridge running lengthwise along midline (Fig. 4A). Sutural ridge with two projections most visible at posterior end of side-on myxospore (Fig. 4A). Projections run lengthwise proximal to surface of frontal-view myxospore (Fig. 4A). Mature myxospore with 2 pyriform, equal sized and symmetrical polar capsules 7.0–8.2 µm long (7.6 ± 0.6; n = 50), 2.3–2.9 µm wide (2.6 ± 0.3; n = 50); polar filament with 8–9 turns in coil (Figs. 3 and 4). Basal sporoplasm located within posterior third of myxospore, containing one or two nuclei and large iodinophilous vacuole (Figs. 3 and 4A). Mucus coat enveloping posterior two-thirds of myxospore, obvious in stained wet mounts (Fig. 3A) and TEM preparations (Fig. 4A). Morphology of presporogonic stages in fathead minnows or *Tubifex* were not assessed.

3.1.2. Molecular and phylogenetic characterization

BLASTn search of the 18S rDNA *M. rasmusseni* n. sp gene sequence in GenBank showed that it was dissimilar to all other submitted myxozoan sequences. When entered into GenBank, the *M. rasmusseni* n. sp. sequence was most similar to the newly-described *M. carlhubbsi* from the gills of southern striped shiners from Arkansas, USA (McAllister et al., 2023, 95.2%), and *M. bilobus* from golden shiner in Ontario, Canada (Cone et al., 2005; DQ008579, 92.2%). The *M. rasmusseni* n. sp. 18S rDNA sequence aligned up to 97% with other *Myxobolus* spp. most of which are associated with infection of the gill lamellae and filaments of cyprinid fishes (Fig. 5; Supplementary Table 1). This group included *M. bilobus* (Cone et al., 2005), *M. pseudokoi* (Li and Desser, 1985), and *M. carlhubbsi* (McAllister et al., 2023), forming a monophyletic clade of cyprinid-infecting species from North America (Fig. 5). This clade was sister to a clade of cyprinid-infecting species mostly from Europe with the exception of *Myxobolus* sp. EzoUgui (Yustinasari et al. unpublished; LC544125, 93.1%), *M. obesus* (Gurley, 1893), *M.* Hungary-EE-2003, (Eszterbauer et al., 2015), *M. eirasianus* (Cech et al., 2012), *M. intimus*

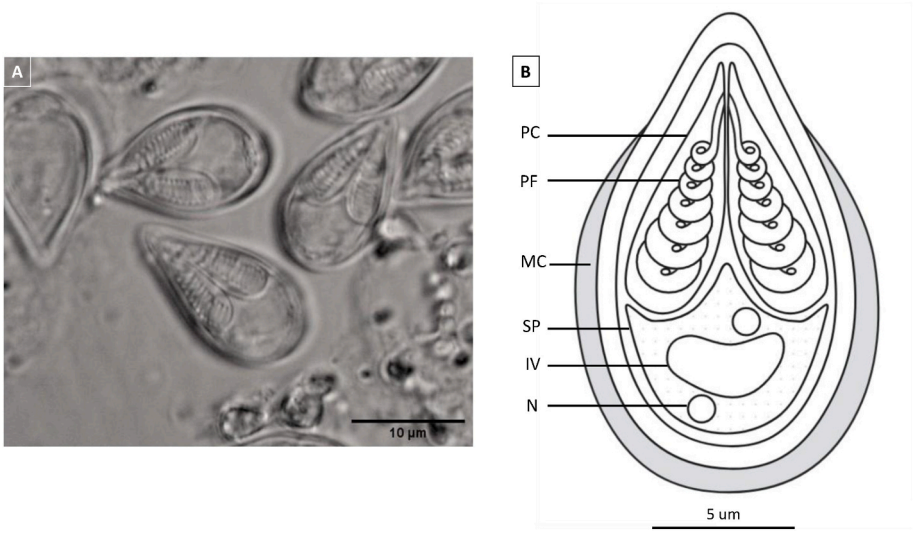

Fig. 3. A. Myxospores of *Myxobolus rasmusseni* n. sp. prepared from a wet mount of a plasmodia-packed lesion located in the circumorbital cavity of an infected fathead minnow. A. Myxospores imaged with differential interference contrast microscope. Thin mucus coat envelopes posterior two thirds of myxospores. B. Composite line drawing of a *Myxobolus rasmusseni* n. sp. myxospore; PC – polar capsule; PF – polar filament; MC – mucus coat; SP – sporoplasm; IV – iodinophilous vacuole; N – nucleus.

(Cech et al., 2012) *and M. dujardini* (Mitchell et al., 1985).

3.1.3. Remarks

In addition to RNA gene sequence dissimilarities, the new species is distinguished from its closest relatives *M. pseudokoi* (Li and Desser, 1985), *M. bilobus* (Cone et al., 2005), and *M. carlhubbsi* (McAllister et al., 2023) in host tissue site selection within the head cavities and in myxospore morphology. Individual plasmodia of each of the other clade members infect the gills. Furthermore, *M. rasmusseni* n. sp. is the only species in the clade whose pattern of development leads to large, conspicuous host lesions that are filled with multiple myxospore-filled plasmodia.

Myxospore metrics of the 22 *Myxobolus* spp. that infect cyprinid hosts (Fig. 5) overlap with the new species (Table 2). However, *M. rasmusseni* n. sp. myxospores are longer and wider than *M. carlhubbsi* and *M. pseudokoi* and smaller than *M. bilobus* (Table 2). Myxospores of the new species has uniform-shaped polar capsules that are longer than the polar capsules of *M. pseudokoi* and *M. carlhubbsi*, the latter of which has irregular-shaped polar capsules. Further, *M. bilobus* has longer and irregular-sized polar capsules compared to the other 3 species in the clade. *Myxobolus rasmusseni* n. sp. has 8 to 9 coils in its polar filaments, whereas *M. pseudokoi* has 6–7 and *M. carlhubbsi* has 6 to 11 coils. The new species has a distinct sutural ridge along the midline lengthwise of the myxospore that has additional projections running adjacent on each side (Fig. 4A). In contrast, the sutural ridge on myxospores of *M. carlhubbsi* lack additional projections along the ridge, and *M. bilobus* has no sutural ridge. Ridge structure on *M. pseudokoi* myxospores is unknown. Finally, *M. rasmusseni* n. sp. has a distinct posterior iodinophilous vacuole located within the sporoplasm, similar to *M. pseudokoi*, whereas *M. bilobus* and *M. carhubbsi* lack a vacuole.

Myxobolus rasmusseni n. sp. occupies a separate branch from the sister taxa, *M. pseudokoi* and *M. carlhubbsi*. The node that distinguishes these 3 taxa has 100% bootstrap support (Fig. 5). Furthermore, the branch length for *M. rasmusseni* n. sp. is longer than the length of the *M. carlhubbsi* and *M. pseudokoi* branch. The greater morphological outlier in this clade, *M. bilobus*, branches separately from the others with bootstrap support of 77% and longer branch length. The new species shares the highest percent sequence similarity with *M. pseudokoi*, at 95.2%, whereas other distinct species on the phylogenetic tree share greater sequence similarity, for example *M. obesus* and *M.* sp. Hungary-EE-2003 at 97.1% (Supplementary Table 1). Unfortunately, the single sequence available on GenBank for *M. pseudokoi* is less than half of the bp length (n = 1967) available for the *M. rasmusseni* n. sp. sequence.

Several *Myxobolus* spp. are reported from fathead minnows or hosts in the genus *Pimephales* but for which no sequences are available. *Myxobolus hyborhynchi* Fantham, Porter, and Richardson 1939 is described from bone and cartilage tissue of the head, pectoral, and caudal fins of fathead minnows (Fantham, Porter and Richardson, 1939; Cone and Frasca, 2001) but this species is not coelozoic within the head cavities and does not develop the lesions that characterize infections with *Myxobolus rasmusseni* n. sp. Myxospore, polar capsule, and mucus coat characteristics also differ between the two species (Table 2). Plasmodia of *Myxobolus mutabilis* Kudo (1934) infects the integument of the head and fins of *P. notatus*. Its myxospores are ellipsoidal to spherical in shape, in stark contrast to the uniformly pyriform myxospores of *M. rasmusseni* n. sp. Similarly, myxospores of *M. angustus* Kudo (1934) of the gill filaments and lamellae of *P. promelas, P. vigilax, and P. notatus* (Table 2; McAllister et al., 2023) are slightly shorter compared to *M. rasmusseni* n. sp. and have asymmetrical polar capsules (Table 2). Lastly, *M. hendricksoni* Mitchell et al. (1985) resides within brain tissue of *P. promelas* but has spherical/ellipsoidal myxospores, with shorter polar capsules and fewer polar filament coils (Table 2).

3.2. Gross observations of lesion-bearing fathead minnows

Conspicuous, whitish, and approximately circular lesions were a common outcome of infection with *M. rasmusseni* n. sp. Lesions were most obvious around the circumorbital sinus and the epithelial tissues of the opercula and pectoral girdle (Fig. 1BC, 2, Supplementary Content Video). Exophthalmia of the circumorbital sinus was asymmetric (Fig. 1A–C), evident as distension or distortion of the region encircling both eyes, especially on the dorsal surface (Fig. 1BC, 2). Lesions were associated with disfigurement of the eye and circumorbital sinus, including hemorrhage around an eye in one infected fish (Fig. 1D) and eye ablation in another (Fig. 1E). Our anecdotal observations of large numbers of lesion-bearing fathead minnow indicated that lesions were frequently associated with structural changes to the mouth, mandibles, and the oral and olfactory chambers. Further, lesions occupying the retroorbital and circumorbital spaces were frequently associated with distortion to the circumorbital skeleton.

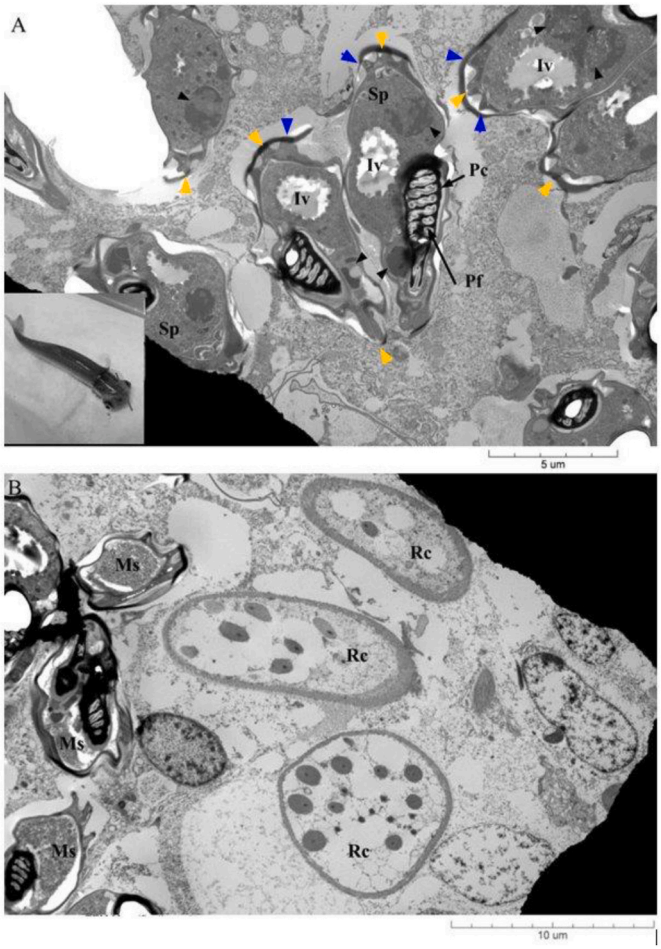

Fig. 4. Transmission electron micrographs of plasmodia that contain *M. rasmusseni* n. sp. myxospores. Sections are from lesioned tissue (see inset in A) located in the circumorbital cavity of a fathead minnow. A. Side-on view of a couplet of *Myxobolus rasmusseni* n. sp. myxospores at 2500X magnification. Sp - Sporoplasm, Iv - Iodinophilous vacuole, Pc - Polar capsule, Pf - Polar filament; Black arrowheads indicate nuclei, orange arrowheads indicate sutural ridge along the midline of myxospore; blue arrowheads indicate posterior projections on the myxospore. B. Myxospores sectioned in various orientations with adjacent rodlet cells at 2000X magnification. Rc - Rodlet cell, Ms: myxospore.

3.3. Histology of the host-parasite interface

Numerous discrete myxospore-containing plasmodia were visible within stained and unstained histological sections of head cavities of lesion-bearing fathead minnows (Figs. 6 and 7). Plasmodia were asymmetrical, highly variable in size and enveloped by a thin-walled membrane (Figs. 6 and 7). Individual plasmodia were filled with stained and unstained myxospores (Fig. 7 insert). Clusters of plasmodia filled the entire volume of the cranial cavity of lesion-bearing fathead minnows with extensions anteriorly into the nasal cavity, posteriorly into the brain cavity (and associated ventricles), and laterally between the two orbital cavities (Fig. 5). The outer membrane of peripheral plasmodia was in direct physical contact with host neural, muscular, and connective tissues (Fig. 6). Neither plasmodia nor myxospores were observed within host tissues. A thin-walled membrane was continuous around the circumference of some plasmodia (Fig. 7). In cases where the membrane was discontinuous, the contents of adjacent plasmodia appeared to be shared. The membrane surrounding plasmodia in the region between the optic lobes of an infected fathead minnow was continuous with the membrane that enveloped a single co-infecting metacercariae of the trematode *Ornithodiplostomum ptychocheilus* (Fig. 7). Rodlet cells were frequently observed adjacent to myxospores in TEM preparations (Fig. 4B).

3.4. Evidence of the Myxobolus rasmusseni n. sp. life cycle

18S rDNA gene sequences amplified from the 10 TAM-releasing oligochaete worms corresponded to two species of annelid in the family Tubificidae. Sequences from 8 of the 10 worms were 96–99% similar to known sequences of *Ilyodrilus templetoni,* and 2 of the 10 were 100% similar to *Tubifex*. Both myxozoan DNA sequences were compared against the sequence generated for *M. rasmusseni* n. sp. and to other sequences available in GenBank. The myxozoan 18S rDNA gene sequences (PP591956) recovered from the two *T. tubifex* worms were a 100% match with the consensus sequence of *M. rasmusseni* n. sp. myxospores from fathead minnows. The closest match (93–94%) in 18S rDNA sequences (PP951958) recovered from triactinomyxon spores released from each of the 8 *I. templetoni* worms were to *Dicauda atherinoidi* (Loch et al., 2017), a myxozoan of the head region of emerald and mimic shiners in North America.

3.5. Seasonality of lesion development

There was high variation in the proportion of fathead minnows that contained visible lesions between the three sampling periods and between the two sites (Fig. 8). *Myxobolus rasmusseni* n. sp. lesions were virtually absent in all 3-4-mo old young-of-the-year fathead minnows (Total n = 100) collected in September 2020 (Fig. 8). The exception was a large young-of-the-year from Coalhurst Stormwater Pond in June 2021. In contrast, all 1-yr old, June-collected fathead minnows from Coalhurst Stormwater Pond had characteristic lesions on the head region whereas lesions were absent in 1-yr old fathead minnows from McQuillan Reservoir sampled at the same time (Fig. 8). Four months later, lesions were present in 29.4% and 85.5% of 16 mo old fathead minnows sampled from McQuillan Reservoir and Coalhurst Stormwater Pond, respectively.

4. Discussion

The myxospores of *Myxobolus rasmusseni* n. sp. have distinct dimensions, they develop within multiple plasmodia in sites other than the host's gills, and plasmodia development is associated with conspicuous lesions that are distinct from other species of myxozoans, including those that infect related cyprinid fishes. The results of our maximum likelihood analysis placed *Myxobolus rasmusseni* n. sp. as sister to a group of three other *Myxobolus* spp. that infect North American cyprinids. This clade was itself placed within a larger group of mostly European *Myxobolus* spp. of cyprinid fish. Overall, the phylogeny is closely congruent with others that describe a well-supported clade involving cyprinid-infecting *M. pseudokoi*, *M. bilobus*, and *M. carlhubbsi* that is placed within a clade of primarily European *Myxobolus* spp. (Cone et al., 2005; McAllister et al., 2023). The combined evidence from interspecific morphological comparisons, patterns of within-host development, the presence of conspicuous epidermal lesions, and the results from comparative 18S rDNA gene sequences support the new-species designation for *M. rasmusseni* n. sp.

Host lesions associated with the development of the plasmodia stages of myxozoans have been reported within species-specific locations in the skin, muscle, viscera, and especially gill filaments for other *Myxobolus* spp. in a range of freshwater and marine fishes (e.g. Loch et al., 2017). As in these other descriptions, lesions associated with the development of *M. rasmusseni* n. sp. are filled with one to numerous plasmodia that in turn are filled with mature myxospores. Our observations of whole-head histological sections indicated that myxospore-containing plasmodia were not restricted to the conspicuous epidermal lesions. Rather, fathead minnows that had lesions surrounding the eyes for example, also contained numerous plasmodia that filled the entire cranial cavity.

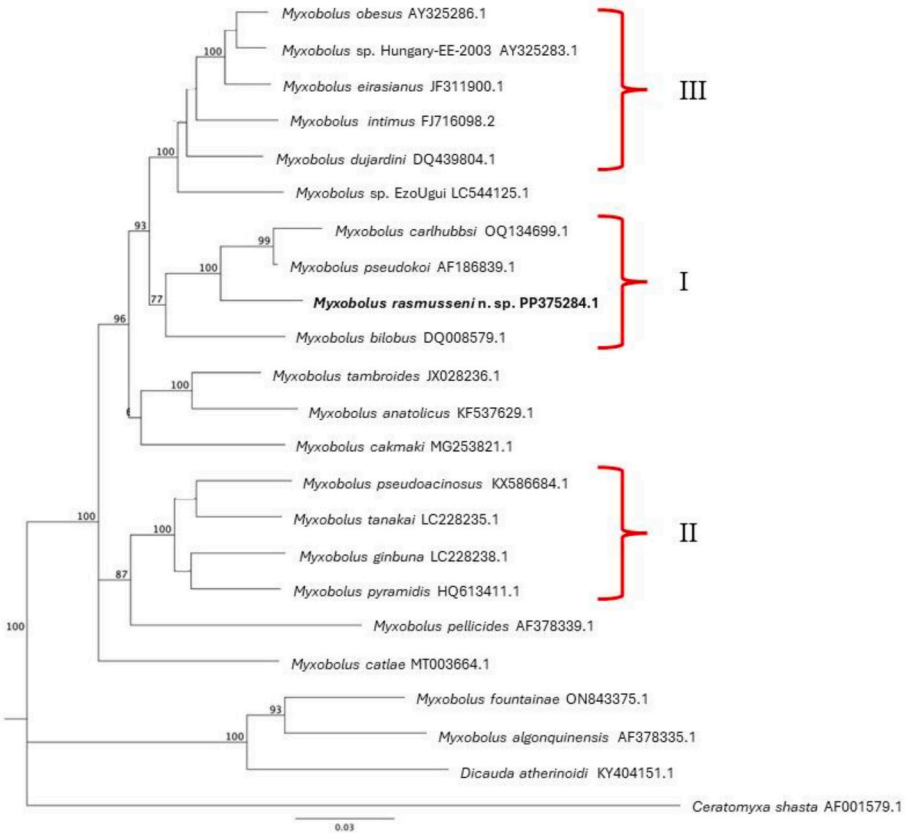

Fig. 5. Phylogenetic tree produced by Bayesian analysis of aligned partial 18S rDNA gene sequences of *M. rasmusseni* n. sp. and other *Myxobolus* spp. infecting cyprinid fishes in Canada, Europe, and Asia. The tree is rooted with *Ceratonova shasta* (AF001579.1). Nodes are denoted with bootstrap probabilities generated by Bayesian analyses. Species in taxa in groups I-III are highlighted in the pairwise percent identity matrix in Supplementary Table 1.

Table 2
Comparative myxospore morphometrics for *Myxobolus rasmusseni* n. sp. and related *Myxobolus* spp. All metrics provided in um.

Species	Host species	Site	Length	Width	PCL	PCW	PFC	Reference
Myxobolus rasmusseni	*Pimephales promelas*	head	15.1 ± 0.4	7.6 ± 0.4	7.6 ± 0.6	2.6 ± 0.3	8–9	This study
Myxobolus carlhubbsi	*Luxilus chrysocephalus isolepis*	gills	12.7 ± 0.4	6.1 ± 0.3	6.4 ± 0.3, 6.2 ± 0.3		6–11	McAllister et al. (2023)
Myxobolus bilobus	*Notemigonus crysoleucas*	gills	21 ± 0.6	8.4 ± 0.5	10.8 ± 0.7, 10.1 ± 0.7	2.7 ± 0.2, 2.8 ± 0.2	7–9	Cone et al. (2005)
Myxobolus pseudokoi	*Notropis cornutus*	gills, skin	13.5	6.5	6.5	2.5	6–7	Li and Desser, 1985
Myxobolus dujardini	*Leuciscus, Leuciscus cephalus, Rutilus, Cyprinus carpio, Perca fluviatilis, Scardinius erythrophthalmus*	gills	11.5 ± 0.4	7.4 ± 0.6	5.5 ± 0.5	2.3 ± 0.4	n.d.	Cech et al., 2012; Molnar et al. (2006)
Myxobolus angustus	*Pimephales vigilax*	gills	14–15	7–8	8–9.5	2.5-3.0	n.d.	Kudo (1934)
Myxobolus sp. *cf. angustus*	*Pimephales vigilax, Pimephales notatus, Pimephales promelas*	gills	12.9 (12.3–14.4)	7.5 (6.7–8.2)	7.9(7.2–9.0), 7.6(7.2–8.5)	3.2(2.8–3.5), 3.1(2.8–3.6)	n.d.	McAllister et al., 2023
Myxobolus hendricksoni	*Pimephales promelas*	brain	13.1 (11–15.5)	12.3 (10–15)	6.6 (6–7.5)	3.6 (3.4–4)	4–6	Mitchell et al. (1985)
Myxobolus hyborhynchi	*Hyborhynchus notatus*	mandible	9.1–10.9	7.3–8.6	4.1–5.9	2.3-2.5	n.d.	Fatham et al., 1939
Myxobolus hyborhynchi	*Pimephales promelas*	head, bone, cartilage	11–12.5	8–9.5	5–6.5	2.5-3.0	5–6	Cone and Frasca, 2001
Myxobolus mutabilis	*Pimephales notatus*	head, integument	9.5–12	7.5–9	5–6.5	2–3.5	n.d.	Kudo (1934)
Myxobolus tambroides	*Tor tambroides*	gills	9.9 ± 0.4	7.4 ± 0.2	5.7 ± 0.8	2.6 ± 0.2	5–6	Székely et al., 2015
Myxobolus tanakai	*Cyprinus carpio*	gills	15.4–18.6	6.3–8.4	7.6–9.4	2.0–2.7	8–10	Kato et al., 2017

PCL = polar capsule length; PCW = polar capsule length; PFC – number of polar filament coils, n.d. – not determined.

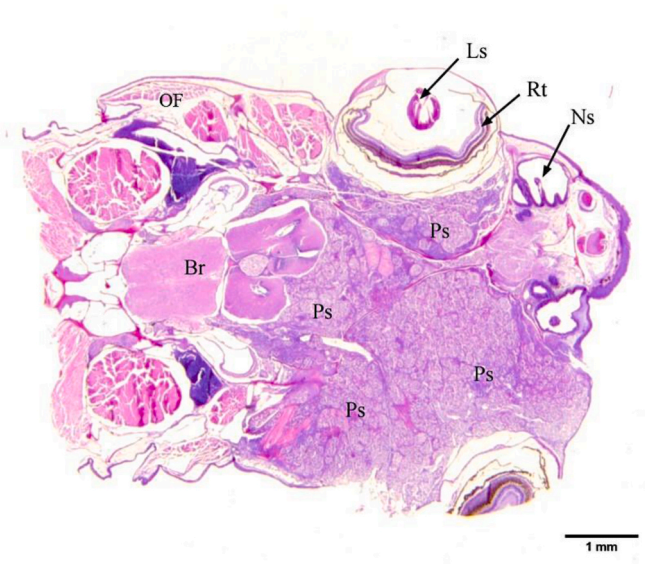

Fig. 6. Coronal histological section through the dorsal head region along the frontal plane of a fathead minnow that contained multiple, various-sized plasmodia of *Myxobolus rasmusseni* n. sp. 1.25X magnification. Rt - Retina of the eye, Ps - Plasmodia, Br - Brain, Ls - Lens of the eye, Ns - Nares, Of – Opercular flap.

Indeed, the large mass of contiguous plasmodia appears to extend into all available space within the cranial cavity, including into the ventricles of the brain and including into the eye orbits. These histological observations of lesions, combined with the results of the longitudinal host survey, support the idea that the lesions in fathead minnows arise from the development of coelozoic plasmodia within the cranial cavity of the host over the course of at least 12 mos.

We did not observe *M. rasmusseni* n. sp. plasmodia or myxospores within host tissue. Tropism within muscle, vascular, bone, and other fish tissue is a common finding for other *Myxobolus* spp., including for those of the central nervous system in fathead minnows (Mitchell et al., 1985; Cone and Frasca, 2002) and other cyprinid hosts (Khoo et al., 2010). Although these contrasting results may arise from the limited scale of our histological sampling, coelozoic development of plasmodia, especially within the head cavity and brain case, appears to be a characteristic feature of the interaction between *M. rasmusseni* and its host. Coelozoic development of plasmodia, either through the multiplication of individual plasmodia, or an increase in the volume of individual plasmodia (or both), provides a parsimonious explanation for the filling of the cranial cavity that we observed in whole-head histological sections. Our observation of large numbers of rodlet cells adjacent to myxospores supports the notion that aspects of the host's inflammatory response (Manera and Dezfuli, 2004; Matisz et al., 2010) may also be involved in lesion development. Thus, coelozoic development of plasmodia within the head cavity, possibly in combination with aspects of host inflammation defenses, may result in the conspicuous exopthalmia around the eyes, and to the other 'bulging' lesions that were observed around the nares, operculum, and oral cavities.

The transport of myxospores across the thin membrane that surrounds peripheral plasmodia within epidermal lesions could lead to the expulsion of infective myxospores directly into the water column. This possibility would be enhanced in mid-to late-summer when inflammation-induced lesions, especially surrounding the host's eyes, are most obvious. If so, transmission of viable myxospores into *T. tubifex* could occur in the absence of the death (e.g. via predation) of infected fathead minnows. The shedding of myxospores through myxozoan-induced lesions has been suggested for some bone-dwelling species such as *M. hyborhynchi* in fathead minnows (Cone and Frasca, 2002) and *M. artus* in carp (Ogawa et al., 1992). Determining a role for myxospore shedding in transmission requires more detailed histological approaches, and ideally, controlled exposures involving naïve *T. tubifex* in water containing fathead minnows with lesions versus fathead minnows without lesions.

The results of our periodic sampling of the 2020 fathead cohort provides an estimate for the timing of initial TAM exposure and the rate of development of plasmodium-filled lesions. Only one of the 100 3–4 mo old fathead minnows sampled in September 2020 contained lesions. In stark contrast, each of the 50 1-yr old juveniles from this cohort sampled at Coalhurst Pond had lesions. Since peak release of TAM's into the water column from *T. tubifex* occurs in June/July (Tilley, 2021), it is unlikely that the 100% prevalence of lesions in juveniles in June 2021 can be explained by exposure earlier that spring. The implication is that all 0+ aged fathead minnows at Coalhurst Pond were exposed to TAM's during their first few months of life and that plasmodia development to the lesion stage requires a minimum of 12 mo. This initial estimate of the timing of myxospore development within the vertebrate host is consistent with the results of laboratory exposures involving other species in the genus *Myxobolus* (Feist et al., 2015). Information on the nature of development of pre-sporogonic stages in fathead minnows is an important direction for future studies.

The results of our cohort analysis also showed that patterns of TAM

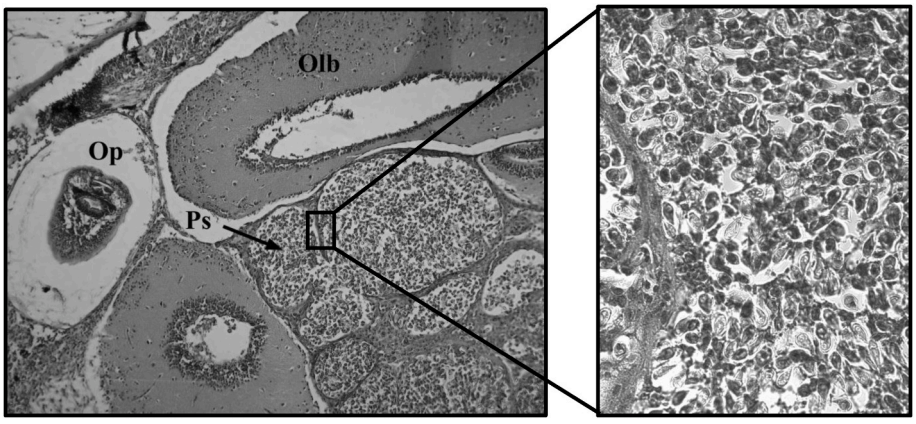

Fig. 7. Coronal histological section of the anterior head region of a *Myxobolus rasmusseni* n. sp. infected fathead minnow. Approximately 8 myxospore-filled plasmodia are located between the two optic lobes in the anterior-dorsal region of the head cavity. Plasmodia demarcated from adjacent host tissue by a thin fibrocytic membrane that also encircles *Ornithodiplostomum ptychocheilus* metacercariae. 100X magnification. Op = *Ornithodiplostomum ptychocheilus* metacercariae, Olb: Optic lobe of the minnow brain, Ps: Plasmodia of *Myxobolus rasmusseni* n. sp. Inset demonstrates distribution of numerous stained and unstained myxospores located within plasmodia.

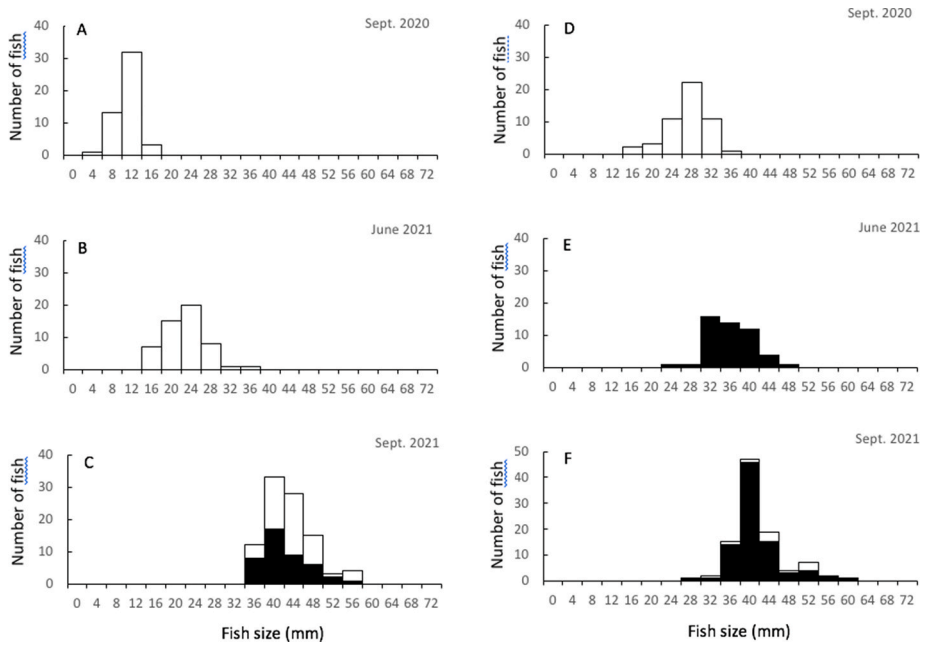

Fig. 8. Size-frequency distributions of fathead minnows collected from two wetlands in southern Alberta. The left-hand triplet of graphs (A, B, C) indicates size distributions of the 2020 cohort of fathead minnows assessed in Sept. 2020, June 2021, and Sept. 2021 at McQuillan Reservoir. The right-hand triplet (D, E, F) indicates size distributions assessed at the same times for Coalhurst Stormwater Pond. Dark bars indicate minnows with *M. rasmusseni* n. sp. lesions.

transmission into fathead minnows and subsequent patterns of lesion development differed markedly between the two sites. In contrast to the pattern of exposure and development described above for fathead minnows in Coalhurst Pond, lesions were not observed in samples from McQuillan Pond until fathead minnows were approximately 16 mo old. Site-specific variation in factors such water temperature, *T. tubifex* density, water depth, substrate characteristics, pond size, and water turbidity could explain these results. One striking difference in the demography of the two fathead minnow populations was the >50% difference in mean size in September-collected 0+ aged fish. One explanation for this result is a delay in hatching date of fathead minnows at McQuillan Pond. Fathead minnows are highly variable in spawning time and those that are hatched in early summer consistently tend to be larger than those spawned later in the summer (Divino and Tonn, 2007). A later hatch date, combined with shorter body lengths during the late summer/early fall transmission window, could explain the delay in lesion development in fathead minnows at McQuillan Pond relative to those in Coalhurst Pond.

The complete life cycles of *Myxobolus* spp. have been established for only approximately 5% of the described species in the genus (Eszterbauer et al., 2015). Our results establish the likely life cycle of *M. rasmusseni* n. sp. within University Pond. DNA sequences amplified from plasmodia-containing lesions of infected fathead minnows were an identical match to the sequences amplified from syntopic TAM-releasing *T. tubifex*. Although life-cycle confirmation is a key advance in studies of myxozoans, our identification of *T. tubifex* as a required host for the sexual stages of *M. rasmusseni* n. sp. is not surprising. *Tubifex*/fish life cycles have been described for other species in the genus *Myxobolus*, including whirling-diseasing causing *M. cerebralis* (Lom and Dykova, 2006; Eszterbauer et al., 2015). Unfortunately, our efforts to further confirm the life cycle by exposing egg-reared juvenile fathead minnows to the matching TAMs were interrupted by Covid-19 restrictions in Fall 2020.

The introduction and establishment of *M. rasmusseni* n. sp. in University Pond and other sites in southern Alberta highlights the ability for myxozoans to rapidly colonize disconnected habitats. University Pond was developed as an anthropogenic habitat feature associated with the construction of the Alberta Water and Environmental Science Building in 2009 on the University of Lethbridge campus. The pond was drained in 2015 to accommodate repairs to the lining of the pond. Fathead minnows recolonized the pond one year later. The lesions associated with the development of *M. rasmusseni* n. sp. pseudocysts were first observed in one-year old fathead minnows in 2017. This sequence of wetland development requires that the 0+ aged fathead minnows from the 2016 cohort were exposed in the same summer that the wetland was filled. This, in turn, requires that either infected *T. tubifex* or infective myxospores survived the draining process in 2015, or that the oligochaetes were exposed to infective stages in the same year that the pond was filled. Regardless of which of these scenarios occurred, *M. rasmusseni* n. sp. established in both of its required hosts within a single year of the colonization of the pond by fathead minnows and has persisted in the fathead minnow and worm population since. The establishment of *Dicauda* sp. in the other species of oligochaete that occurs in the pond, *Ilyodrilus templetoni,* further confirms the remarkable ability of myxozoans to rapidly colonize freshwater habitats.

Emerging infectious diseases are defined as pathogens that have either experienced expansion in incidence or geographic range or have recently been discovered or have undergone a shift into a new species of host (Daszak et al., 2001). The detection of *M. rasmusseni* n. sp., in fathead minnows from multiple waterbodies since 2017 where it had not been detected before suggests that it is emerging in fathead minnow populations in southern Alberta. Previous host surveys involving >2000 complete necropsies of individual fathead minnows have occurred at these same sites for over 20 years (Sandland et al., 2001; Ahn, 2019; Hirtle et al., 2023). In addition, intensive annual host surveys have occurred at two of these sites (Ahn, 2019), one of which has contained juvenile fathead minnows with *M. rasmusseni*-induced lesions since 2017. Given the cryptic nature of myxozoans in general, particularly involving their microscopic myxospores within host tissues, under-reporting should be expected. Yet the conspicuous nature of plasmodia-packed lesions on the head and body and the persistence of the deformities makes it unlikely that infection would be missed. Although we recognize that direct demonstration of myxozoan emergence is difficult (review by Hallett et al., 2015), our evidence from host surveys across broad temporal and spatial scales support the idea that *M. rasmusseni* n. sp. is an emerging parasite of this important species of

forage fish. Unfortunately, the origin of *M. rasmusseni* n. sp. in fathead minnows is unknown. Furthermore, there is no information available regarding infection in other species of cyprinid that are sympatric at sites where *M. rasmusseni* n. sp. occurs in fathead minnows. Inter-basin transfer of numerous fish species (including various cyprinids) and their parasites, is certainly possible through the extensive irrigation network that connects large numbers of waterbodies in southern Alberta. Thus, there is potential for host shifts involving myxozoans and other parasites. Understanding the incidence, causes, and consequences of emergence of myxozoans in this and other freshwater ecosystems is an important direction for future studies.

Financial support

This research was supported by the National Scientific and Engineering Research Council of Canada (CG) and the Alberta Conservation Association (Grants in Biodiversity to MT).

Declarations of interest

None.

Ethical standards

Animal collections were approved by Alberta Environment and Parks (permit nos. 20–2402, 21–2404, and 22–2401) and animal handling was approved by the University of Lethbridge Animal Welfare Committee (protocol #1806) in adherence with guidelines established by the Canadian Council on Animal Care.

CRediT authorship contribution statement

Molly F. Tilley: Writing – original draft, Visualization, Validation, Methodology, Formal analysis, Data curation, Conceptualization. **Danielle Barry:** Writing – original draft, Validation, Methodology, Investigation, Formal analysis, Data curation. **Patrick C. Hanington:** Writing – review & editing, Methodology, Formal analysis, Data curation, Conceptualization. **Cameron P. Goater:** Writing – review & editing, Writing – original draft, Supervision, Resources, Project administration, Funding acquisition, Data curation, Conceptualization.

Acknowledgements

We thank Micky Ahn and Cash Jackson for assistance with fieldwork and Alyssa Turnbull for technical assistance in the lab. We also thank Lauren Edison for her help preparing figures, Andy Hurly for photographing infected minnows, and Theresa Burg and two anonymous reviewers for sharing their expertise. We extend thanks to David Cone for direction and assistance throughout all stages of this work.

Appendix A. Supplementary data

Supplementary data to this article can be found online at https://doi.org/10.1016/j.ijppaw.2024.100944.

References

Ahn, S., 2019. Effects of host community structure on parasite transmission and disease risk. Master of Science. University of Lethbridge.

Atkinson, S.D., Bartosova-Sojkova, P., Whipps, C.M., Bartholomew, J.L., 2015. Approaches for characterizing myxozoan species. In: Okamura, B., Gruhl, A., Bartholomew, J. (Eds.), Myxozoan Evolution, Ecology and Development. Springer, International, pp. 111–124.

Barta, J.R., Martin, D.S., Liberator, P.A., Dashkevicz, M., Anderson, J.W., Feighner, S.D., Elbrecht, A., Perkins-Barrow, A., Jenkins, M.C., Danforth, H.D., Ruff, M.D., Profous-Juchelka, H., 1997. Phylogenetic relationships among eight *Eimeria* species infecting domestic fowl inferred using complete small subunit ribosomal DNA sequences. J. Parasitol. 83, 262–271.

Bartasova, p., Fiala, I., Hypsa, V., 2009. Concatenated SSU and LSU rDNA confirm the main evolutionary trends within myxosporeans (Myxozoa: myxosporea) and provide an effective tool for their molecular phylogenetics. Mol. Phylogenet. Evol. 53, 81–93.

Bartholomew, J.L., Kerans, B., 2015. Risk assessments and approaches for evaluating myxozoan disease impacts. In: Okamura, B., Gruhl, A., Bartholomew, J. (Eds.), Myxozoan Evolution, Ecology and Development. Springer, International, pp. 379–396.

Carraro, L., Bertuzzo, E., Mari, L., Fontes, I., Hartikainen, H., Strepparava, N., et al., 2017. Integrated field, laboratory, and theoretical study of PKD spread in a Swiss pre-alpine river. Proc. Natl. Acad. Sci. USA 114, 11992–11997.

Chang, E.S., Neuhof, M., RubInstein, N.D., Diamant, A., Philippe, H., Huchon, D., Cartwright, P., 2015. Genomic insights into the evolutionary origin of the Myxozoa within Cnidaria. Proc. Nat. Acad. Sci. 112, 14912–14917.

Cone, D.K., Frasca, S., 2002. Revised diagnosis, site of development, and lesions due to *Myxobolus hyborhynchi* (Myxozoa) parasitizing fathead minnow in Minnesota. J. Aquat. Anim. Health 14, 209–215.

Cone, D.K., Raesly, R.L., 1995. Redescription of *Myxobolus rhinichthidis* (Myxosporea) parasitizing *Rhinichthys cataractae* with a revised taxonomic list of species of *Myxobolus* known from North American freshwater fishes. Can. J. Fish. Aquat. Sci. 52, 7–12.

Cone, D.K., Yang, J., Sun, G.L., Easy, R., 2005. Taxonomy and molecular phylogeny of *Myxobolus bilobus* n. sp. (Myxozoa) parasitizing *Notemigonus crysoleucas* (Cyprinidae) in Algonquin Park, Ontario, Canada. Dis. Aqu. Org. 66, 227–232.

Daszak, P., Cunningham, A.A., Hyatt, A.D., 2001. Anthropogenic environmental change and the emergence of infectious diseases in wildlife. Acta Trop. 78, 103–116.

Diamant, A., Whipps, C.M., Kent, M.L., 2004. A new species of *Sphaeromyxa* (Myxosporea: Sphaeromyxidae) in devil firefish, *Pterois miles* (Scorpaenidae), from the Northern Red Sea: morphology, ultrastructure, and phylogeny. J. Parasitol. 90, 1434–1442.

Divino, J.N., Tonn, W.M., 2007. Effects of reproductive timing and hatch date on fathead minnow recruitment. Ecol. Fresh. Fish 16, 165–176.

Eszterbauer, E., Atkinson, S.D., Diamant, A., Morris, D.J., EL-Matbouli, M., Hartikainen, H., 2015. Myxozoan life cycles: practical approaches and insights. In: Okamura, B., Gruhl, A., Bartholomew, J.L. (Eds.), Myxozoan Evolution, Ecology and Development. Springer, International, pp. 175–200.

Feist, S.W., Morris, D.J., Alama-Bermejo, G., Holzer, A.S., 2015. Cellular processes in myxozoans. In: Okamura, B., Gruhl, A., Bartholomew, J.L. (Eds.), Myxozoan Evolution, Ecology and Development. Springer, International, pp. 139–154.

Folmer, O., Black, M., Hoeh, W., Lutz, R., Vrijenhoek, R., 1994. DNA primers for amplification of mitochondrial cytochrome c oxidase subunit I from diverse metazoan invertebrates. Mol. Mar. Biol. Biotechnol. 3, 294–299.

Fontes, I., Hallet, S.L., Mo, T.A., 2015. Comparative epidemiology of myxozoan diseases. In: Okamura, B., Gruhl, A., Bartholomew, J. (Eds.), Myxozoan Evolution, Ecology and Development. Springer, International, pp. 317–342.

Frey, K.J., Cone, D.K., Duobinis-Gray, L.F., 1998. *Myxobolus petenensis* n. sp. (Myxosporea) from the circumorbital integument of *Dorosoma petenense* (Clupeidae) in Kentucky Lake. J. Parasitol. 84, 1204–1206.

Hallet, S.L., Diamant, A., 2001. Ultrastructure and small-subunit ribosomal DNA sequence of *Henneguya lesteri* s. sp. (Myxosporea), a parasite of sand whitling *Sillago analis* (Sillaginidae) from the coast of Queensland, Australia. Dis. Aquat. Org. 46, 197–212.

Hallett, S.L., Hartigan, A., Atkinson, S.D., 2015. Myxozoans on the move: dispersal modes, exotic species and emerging diseases. In: Okamura, B., Gruhl, A., Bartholomew, J. (Eds.), Myxozoan Evolution, Ecology and Development. Springer International, pp. 343–362.

Heins, D.C., Baker, J.A., Green, D.M., 2001. Processes influencing the duration and decline of epizootics in *Schistocephalus solidus*. J. Parasitol. 97, 371–376.

Herwig, B.R., Zimmer, K.D., Hanson, M.A., et al., 2010. Factors influencing fish distributions in shallow lakes in prairie and prairie-parkland regions of Minnesota, USA. Wetlands 30, 609–619.

Hirtle, S., Ahn, S., Goater, C.P., 2023. A congeneric and non-randomly associated pair of larval trematodes dominates the assemblage of co-infecting parasites in fathead minnows (*Pimephales promelas*). Parasitol., 150, 1006-1014.

James, C.T., Veillard, M.F., Martens, A.M., et al., 2021. Whirling disease in the Crowsnest River: an emerging threat to wild salmonids in Alberta. Can. J. Fish. Aquat. Sci. 78, 1855–1868.

Khoo, L., Rommel, F.A., Smith, S.A., Griffin, M.J., Pote, L.M., 2010. *Myxobolus neurophilus*: morphologic, histopathologic and molecular characterization. Dis. Aqu. Org. 89, 51–61.

Ksepka, S.P., Rash, J.M., Bullard, S.A., 2022. Two new species of *Myxobolus* (Myxozoa: Myxobolidae) infecting the gills and scales of smallmouth bass. In: Micropterus dolomieu (Centrarchiformes: Centrarchidae) in the French Broad River Basin,. North Carolina. Parasit. Inter., 102615

Kudo, R.R., 1934. Studies on some protozoan parasites of fishes in Illinois. Ill Biol. Monogr. 13, 1–44. University of Illinois.

Liu, Y., Whipps, C.M., Gu, Z.M., Zeng, C., Huang, M.J., 2012. *Myxobolus honghuensis* n. sp. (Myxosporea: bivalvulida) parasitizing the pharynx of allogynogenetic gibel carp *Carrassius auratus gibelio* (Bloch) from Honghu Lake, China. Parasit. Res. 110, 1331–1336.

Loch, T.P., Rosser, T.G., Baumgartner, W.A., Boontai, T., Faisai, M., Griffith, M.J., 2017. New host record and molecular characterization of *Dicauda atherinoidi* Hoffman & Walker 1978. J. Wild. Dis. 40, 1405–1415.

Lom, J., Arthur, J.R., 1989. A guideline for the preparation of species descriptions in Myxosporea. J. Fish. Dis. 12, 151–156.

Lom, J., Dykova, I., 1992. Protozoan parasites of fishes. Dev. Aquacult. Fish. Sci. 26. Elsevier Science Publishers, New York.

Lom, J., Dykova, I., 2006. Myxozoan genera: definition and notes on taxonomy, life-cycle terminology and pathogenic species. Folia Parasitol. 53, 1–36.
Manera, M., Dezfuli, B.S., 2004. Rodlet cells in teleosts: a new insight into their nature and functions. J. Fish. Biol. 65, 597–619.
Markiw, M.E., Wolf, K., 1983. *Myxosoma cerebralis* (Myxozoa: myxosporea) etiologic agent of salmonid whirling disease requires tubificid worms (Annelida: Oligochaeta) in its life cycle. J. Protozool. 30, 561–564.
Matisz, C.E., Goater, C.P., Bray, D., 2010. Density and maturation of rodlet cells in brain tissue of fathead minnows (*Pimephales promelas*) exposed to trematode cercariae. Int. J. Parasitol. 40, 307–312.
McAllister, C.T., Cloutman, D.G., Leis, E.M., Camus, A.C., Robison, H.W., 2023. A new *Myxobolus* (Cnidaria: Myxosporea: Myxobolidae) from the gills of the southern striped shiner, *Luxilus chrysocephalus isolepis* (Cypriniformes: Leuciscidae), from southwestern Arkansas, USA. Syst. Parasitol. 100, 215–229.
Minchew, C.D., 1981. *Unicauda magna* sp. n. (Protozoa, Myxozoa) A new myxozoan from the fin tissues of the fathead minnow, *Pimephales promelas* Rafinesque. J. Fish. Dis. 4, 513–518.
Mitchell, L.G., Seymour, C.L., Gamble, J.M., 1985. Light and electron microscopy of *Myxobolus hendricksoni* sp. nov. (Myxozoa: Myxobolidae) infecting the brain of the fathead minnow, *Pimephales promelas* Rafinesque. J. Fish. Dis. 8, 75–89.
Molnar, K., Marton, Sz, Eszterbauer, E., Szekely, C., 2006. Comparative morphological and molecular studies on *Myxobolus* spp. infecting chub from the River Danube, Hungary, and description of *M. muellericus* sp. n. Dis. Aquat. Org. 73, 49–61.
Nehring, R.B., Thompson, K.G., Shuler, D.L., James, T.M., 2003. Using sediment core samples to examine the spatial distribution of *Myxobolus cerebralis* actinospore production in Windy Gap Reservoir. Colorado. N. Am. J. Fish. Manag. 23, 376–384.
Nei, M., Kumar, S., 2000. Molecular Evolution and Phylogenetics. Oxford University Press, New York, New York, USA.
Ogawa, K., Delgahapitiya, P., Furuta, T., Wakabayayashi, H., 1992. Histological studies on the host response to *Myxobolus artus* Akhmerov, 1960 (Myxozoa: Myxobolidae) infection in the skeletal muscle of carp, *Cyprinus carpio* L. J. Fish. Biol. 41, 363–371.
Okamura, B., Gruhl, A., Bartholomew, 2015. Myxozoan Evolution, Ecology, and Development. Springer International Publishing, Switzerland.
Robinson, C.L., Tonn, W.M., 1989. Influence of environmental factors and piscivory in structuring fish assemblages of small Alberta Lakes. Can. J. Fish. Aquat. Sci. 46, 81–89.
Sandland, G.J., Goater, C.P., Danylchuk, A.J., 2001. Population dynamics of *Ornithodiplostomum ptychocheilus* metacercariae in fathead minnows (*Pimephales promelas*) from four northern-Alberta lakes. J. Parasitol. 87, 744–748.
Székely, C., Borkhanuddin, M., Cech, G., Kelemen, O., Molnar, K., 2015. Life cycles of three *Myxobolus* spp. from cyprinid fishes of Lake Balaton, Hungary involve triactinomyxon-type actinospores. Parasitol. Res. 113, 2817–2825.
Tilley, M., 2021. A new and emerging myxozoan parasite of fathead minnows: species description, life-cycle, and effects to the host. Master of Science. University of Lethbridge.
Wisenden, B.D., Martinez-Marquez, J.Y., Gracia, E.S., McEwen, D.C., 2012. High intensity and prevalence of two species of trematode metacercariae in the fathead minnow (*Pimephales promelas*) with no compromise of minnow anti-predator competence. J. Parasitol. 98, 722–727.